Morphology of a Crystalline/Amorphous Diblock Copolymer: Poly((ethylene oxide)-*b*-butadiene)

Sheng Hong, Lizhang Yang, William J. MacKnight, and Samuel P. Gido*

Polymer Science and Engineering Department, Materials Research Science and Engineering Center, W. M. Keck Electron Microscopy Laboratory, University of Massachusetts, Amherst, Massachusetts 01003

Received January 12, 2001

ABSTRACT: The bulk morphology of a crystalline/amorphous diblock copolymer under different thermal conditions was studied. The diblock copolymer, poly((ethylene oxide)-*b*-1,4-polybutadiene), forms a microphase-separated lamellar morphology in the molten state. For samples crystallized within the range of 20−50 °C, TEM coupled with electron diffraction revealed a microphase-separated, alternating lamellar morphology with the PEO crystalline chains oriented perpendicular to the interface between the PEO and PBD domains. A significant increase in the microphase-separated, lamellar domain spacing was observed upon crystallization. On the length scale of tens of microns, as probed by polarizing optical microscopy, a nonspherultic crystalline texture (with the absence of the Maltese cross), corresponding to the microphase-separated lamellar grain morphology, was observed. In contrast to the integral chain folding observed in PEO homopolymer, the increase in PEO lamellar thickness with decreasing undercooling is continuous in the block copolymer. In addition, the equilibrium melting temperature and lamellar spacing were determined.

Introduction

The morphology of a crystalline/amorphous diblock copolymer poly(ethylene oxide)-*b*-poly(1,4-butadiene) P(EO-*b*-BD) was investigated. Theoretical predictions concerning the morphology of crystalline/amorphous block copolymers have been developed by DiMarzio and co-workers,[1] Whitmore and Noolandi,[2] and Vilgis and Halperin[3] assuming that a thermodynamic equilibrium state can be achieved. The model, shown in Figure 1, assumes a structure of alternating crystalline and amorphous layers. In the crystalline layers there is regular chain folding with the chain stems oriented perpendicular to the interface with the amorphous domains.

Experimental results,[4−21] however, indicated significant deviation from the theoretical model. The morphology of diblock copolymers containing crystallizable blocks was found to be significantly influenced by the crystallization conditions. Depending upon the thermal history and the material properties, either a spherulitic morphology dominated by crystallization or a block copolymer morphology confining the crystalline block into nano scale domains can be formed.[8,9,11] The morphology was thus heavily influenced by kinetics, similar to the case of semicrystalline homopolymers. The parameters controlling the kinetics of the system and thus the morphology formed include the glass transition temperature of the amorphous block, the block copolymer order−disorder transition temperature, and the crystallization temperature.[9,11,20]

For many of the previously studied systems, the domain spacing of lamellar diblock copolymers due to microphase separation is larger than the thickness of chain-folded crystallites which grow inside the microphase-separated layers.[8−12] Therefore, constraints of the preexisting microphase-separated morphology do not limit chain-folded crystallite thickness and have only a modest effect on crystallite orientation.

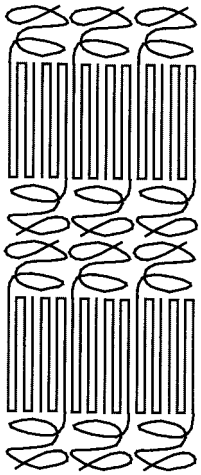

Figure 1. Theoretical model proposed for the structure of symmetric crystalline/amorphous diblock copolymers.[1]

On the other hand, the poly((ethylene oxide)-*b*-butadiene) (P(EO-*b*-BD)) diblock copolymers studied in this report have a smaller lamellar domain size in the microphase-separated amorphous state than the crystalline lamellar long period of PEO homopolymers with similar molecular weight. In addition, it is well known that low molecular weight PEO homopolymer crystals have a characteristic preference for integral chain folding.[22−24] In our previous work,[25,26] we studied the morphological evolution and the influence of dimensional constraint on lamellar domain spacing in thin films of the same P(EO-*b*-BD) material and found, via atomic force microscopy (AFM) and interference optical microscopy, a gradual increase of the melting temperatures and domain spacing with decreasing degree of undercooling. Similar results on P(EO-*b*-hydrogenated 1,2-butadiene) diblock thin films have been reported by

* To whom all correspondences shall be addressed.

10.1021/ma0100596 CCC: $20.00
Published on Web 09/18/2001

Reiter and co-workers.[27] Our thin film results differed from normal low molecular weight PEO crystallization where changes of T_m and crystal long period occurred in discrete steps due to the preference for integral chain folding. Here the study of the effects of microphase-separated confinement upon PEO block crystallization is extended to bulk morphologies of the P(EO-*b*-BD) system.

Experimental Section

P(EO-*b*-BD) was obtained from Polymer Source Inc. It was synthesized via sequential anionic polymerization where polybutadiene (PBD) was polymerized first in cyclohexane. The PBD block has about 69% 1,4 trans structure, 25% 1,4 cis, and about 6% 1,2 structure. The molecular weights and molecular weight distributions of PBD and diblock copolymer were characterized by GPC calibrated with PBD standards. The molecular weight for the PBD block was 5000 g/mol. The molecular weight for the PEO block was calculated from ^{1}H NMR based on the mole ratio of PBD and PEO blocks and was found to be 5600 g/mol. The polydispersity of the diblock copolymer was 1.04. The χN of our system at 80 °C was estimated to be about 70, indicating a relatively strong degree of segregation in the melt state. The density of PBD is 0.94 g/mol,[28] and the densities of crystalline and amorphous PEO are 1.13 and 1.03 g/mol, respectively.[28] These densities allow the calculation of a PEO volume fraction of 51% in the melt state and 48% when crystallized to the degree (88%) indicated by DSC results. The thermal stability of P(EO-*b*-BD) was examined by thermogravimetric analysis (TGA). The sample was held at 150 °C in air for 1 h, and no weight loss was observed. GPC results on the material used in this TGA experiment indicated a slight increase of polydispersity to 1.13. The experiments reported here did not expose the sample to temperatures greater than 90 °C and generally protected the sample from exposure to air. Thus, the copolymer is thermally stable under current experimental conditions without noticeable degradation. To avoid absorption of moisture by PEO, samples were dried under vacuum at 50 °C prior to use, and all the samples were stored under vacuum.

The diblock copolymer was dissolved in toluene and solution cast for a period of 1 week to produce films approximately 1 mm thick. The samples were annealed in a vacuum oven for 2 days, at 90 °C, and then subjected to different thermal treatments in a DSC instrument. Differential thermal analyses were carried out in a Perkin-Elmer DSC-7 equipped with liquid nitrogen cooling. Isothermal crystallization experiments were conducted by heating the sample up to 80 °C and then quickly quenching to the desired crystallization temperature at the maximum speed (−150 °C/min) that can be achieved by the instrument. For experiments using self-seeding methods, the procedures were similar to those described by Kovacs et al.[22] The quantity of the diblock copolymer used in each DSC measurement was 0.8 mg or less. The instrument was calibrated with indium (T_m = 156.6 °C) and eicosane (T_m = 36.44 °C) at the experimental heating rate of 1.0 °C/min on a daily basis. The reproducibility of the melting temperature measured by DSC for identical runs on the same sample was found to be better than 0.1 °C, while for different samples it is better than 0.2 °C.

SAXS data were collected at the Advanced Polymers Beamline (X27C), located at the National Synchrotron Light Source at Brookhaven National Labs (BNL), Upton, NY. Two-dimensional scattering patterns were collected on Fujitsu image plates and then read by a Fujitsu BAS 2000 image plate reader. Custom software at BNL was used to subtract background noise and perform circular averaging. Data were collected for a wavelength of 1.307 Å and a camera length of 1510 mm. SAXS measurements of long periods of samples crystallized at various temperatures were all conducted at room temperature (25 °C). The difference in domain spacing between the crystallization temperature and the lower temperature at which SAXS was run, due to changes in amorphous domain chain conformations, will be very slight.

Samples for optical microscopy were prepared by evaporating 7% toluene solutions of the block copolymer onto a glass cover slide, yielding films approximately 10−100 μm thick. Experiments were conducted using an Olympus BX60F3 optical microscope under cross-polar conditions. Two Mettler FP80 hot stages were used. Samples were held in the melt at 80 °C on one stage and then rapidly transferred to the second stage which was preset to the desired crystallization temperature.

TEM and electron diffraction experiments were conducted on a JEOL 2000 FX-II instrument. The diffraction camera length was calibrated by using an internal gold standard on some of the grids observed. To prepare specimens for TEM, a small piece of copolymer sample was microtomed using a Leica Ultracut Cryomicrotome with a diamond knife at −110 °C to obtain ultrathin (about 40 nm) sections. No solvent or water was used in microtoming and collecting the specimen in order to minimize moisture absorption by the PEO. The thin sections were stained by OsO_4 and observed under TEM. While OsO_4 stains both PBD and PEO, it stains PBD more heavily due to the lack of crystallinity and the presence of unsaturation. Because of the possibility that OsO_4 may disrupt the crystallinity of the PEO block, electron diffraction experiments were conducted on unstained specimens.

Results

Figure 2 shows TEM micrographs of P(EO-*b*-BD) block copolymer that was annealed in the melt at 90 °C and then crystallized at 30 °C. The darker regions are PBD domains that were preferentially stained with OsO_4, while the lighter regions are crystalline PEO domains. It is obvious that the diblock copolymer adopts an alternating lamellar morphology with PEO crystals confined between amorphous PBD layers. WAXS results (not shown) indicated that the PEO in the diblock copolymer had the same monoclinic crystalline structure as formed by PEO homopolymer. As shown in Figure 2a, the sample has good long-range order. However, as shown in Figure 2b, it does display typical block copolymer grain structures,[29,30] suggesting that PEO crystallization occurs within the confinement provided by the preexisting microphase-separated morphology.

The orientation of the PEO crystallites inside the nanoscale domains is determined by TEM and electron diffraction. Figure 3a is an indexed electron diffraction pattern of P(EO-*b*-BD), taken from the region inside the selected area aperture, shown in Figure 3b. The results shown here are from a sample crystallized at 34 °C. However, similar behavior was observed for all samples within the temperature range examined (20−50 °C). To avoid damage to the crystalline structure due to staining, the samples for electron diffraction were not stained. Consequently, the image contrast in Figure 3b is from diffraction contrast and mass thickness contrast arising from the density difference between the crystalline PEO and the amorphous PBD. This contrast is opposite to that of the stained specimens; i.e., dark regions are now PEO domains while the bright regions are PBD domains. Overall, the contrast is much weaker than in the stained samples and disappears within seconds of electron beam exposure. From Figure 3b, the lamellae inside the selected area aperture are observed to all be oriented in approximately the same direction. The diffraction arising from this area (Figure 3a) indicates uniaxial orientation of crystallites with the PEO chain axis perpendicular to the microphase-separated lamellar domains. The 120 reflections are oriented parallel to the lamellar layers in the image, indicating that the [001] crystallographic direction

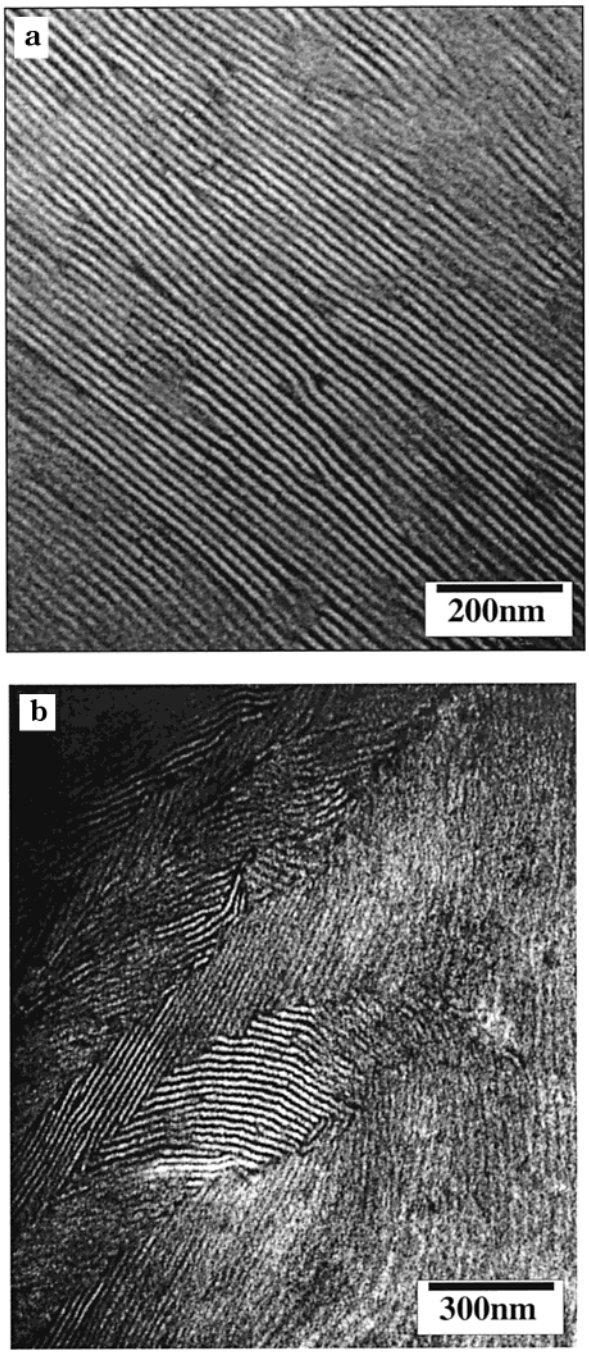

Figure 2. TEM micrographs of P(EO-*b*-BD) sample that was melt annealed and then crystallized at 30 °C.

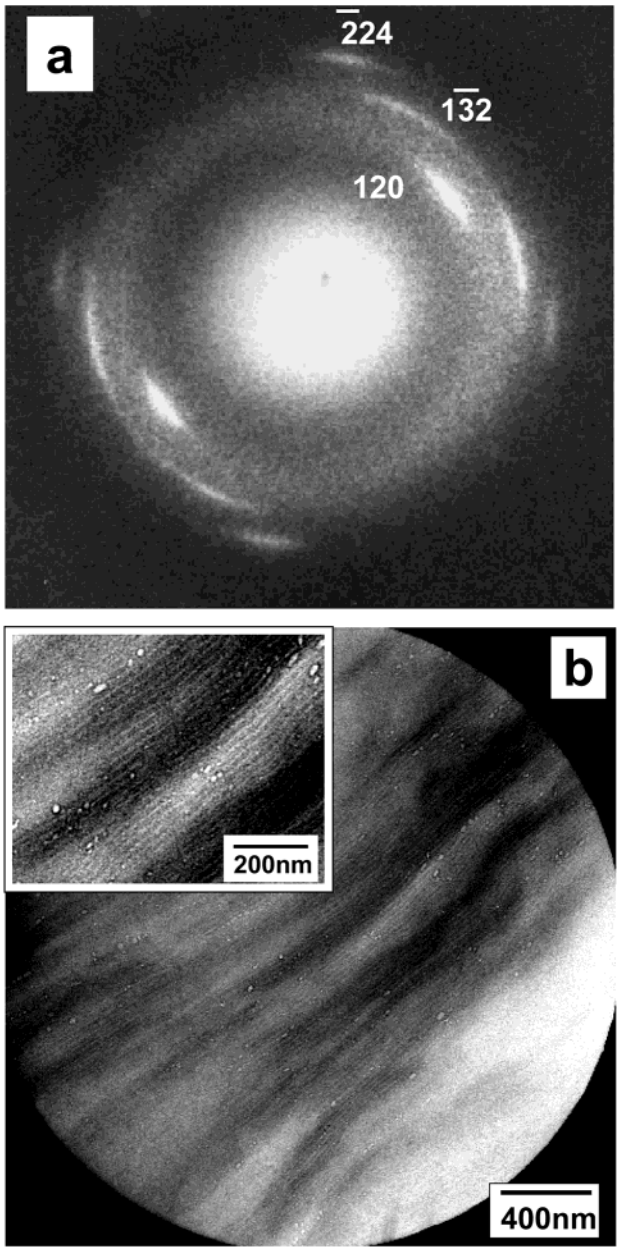

Figure 3. Determination of the orientation of the PEO crystalline chain within the microphase-separated domains. Indexed electron diffraction pattern of P(EO-*b*-BD). TEM micrograph of P(EO-*b*-BD) in selected area aperture.

which is also the chain axis is perpendicular to the layers. The three labeled reflections do not exist in a single planar section through the reciprocal lattice. These reflections intersect the Ewald sphere at the spacings and geometry shown if the PEO reciprocal lattice is rotated around the [001] direction, indicating that the material possesses a fiberlike polycrystalline texture. Generally, the structure of the P(EO-*b*-BD) diblock is similar to that illustrated in Figure 1.

Previously, we observed perfect three-dimensional crystallographic registry between adjacent lamellar layers of P(EO-*b*-BD) block copolymers in thin films containing about six or seven lamellar repeats.[25,26] Our current results for bulk samples indicate only uniaxial alignment of the chain axis normal to the lamellar domains but with rotational disorder of the PEO crystallites around this chain axis direction. The TEM micrographs in Figure 3b show that the orientation of the microphase-separated lamellae is not perfect. The selected area aperture is about 2.5 μm in diameter, and thus the diffraction pattern is collected over a range of lamellar orientations, resulting in the arcing of the reflections observed in Figure 3a. The fact that we are also collecting diffraction data over more than 100 lamellar repeats makes it much less likely that any more highly aligned relationships between adjacent crystalline PEO layers will be detected in the bulk even if such alignments do exist locally within the sample.

To investigate the crystalline morphology of P(EO-*b*-BD) on the length scale of tens and hundreds of microns, sample films were studied by optical microscopy under cross-polar conditions, as shown in Figure 4. The sample was first melted at 80 °C and then crystallized isothermally at various temperatures. Figure 4a was taken

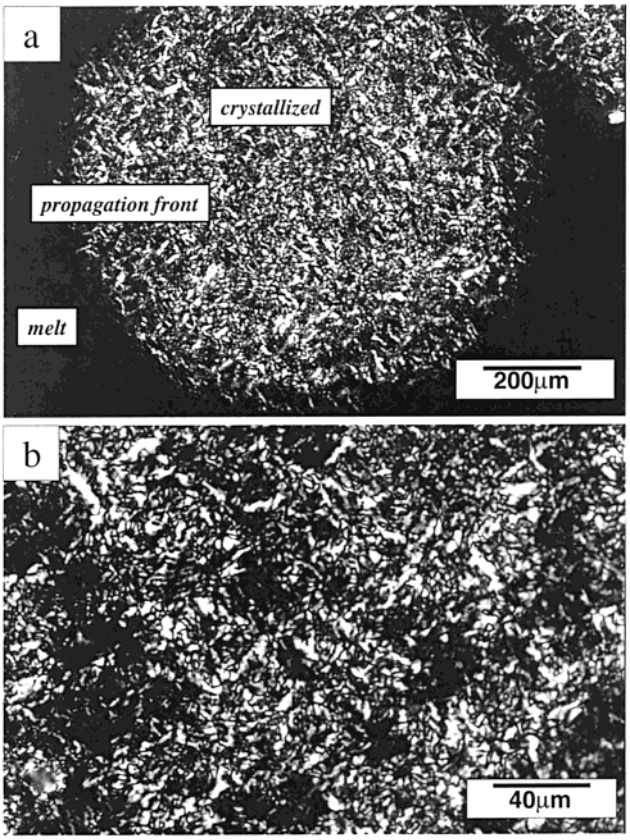

Figure 4. Optical micrographs of P(EO-*b*-BD) under cross-polars. (a) Crystal growth at 45 °C. (b) Enlarged image taken inside the crystallized area in (a).

while the crystallites were still growing at 45 °C. The dark regions correspond to block copolymer in the molten state. The textured bright region contains crystalline PEO and appears to grow from a nucleus located at the center. The lack of any observable texture in the molten region is due to a lack of contrast between PBD and amorphous PEO blocks. Crystallization of PEO in P(EO-*b*-BD) increases the refractive index of the PEO domains and consequently changes the birefringence of the system so that the underlying block copolymer morphology can be seen. Figure 4b shows an enlargement of the texture in the crystalline region, which is due to the grain structures of the microphase-separated block copolymers. Optical images with the same essential features have been reported by Balsara and co-workers[31] in fully amorphous poly(isoprene-*b*-styrene) diblock copolymers.

The bright regions in Figure 4 are grains whose optical axes are oriented at approximately ±45° to the polarizers. These images indicate that the size of the grains of the microphase-separated block copolymer morphology is about 5−20 μm. Figure 4a indicates that the region of PEO crystallization originating from a single nucleus can be 500 μm or larger in diameter. Thus, the growth of crystallites is found to propagate across grain boundaries and to encompass many differently oriented grains. This is possible due to the grain boundary morphologies in microphase-separated lamellar systems which provide for continuity of domain structure across the boundaries.[29,30,32−34]

The crystalline region in Figure 4 does not show the characteristic Maltese cross, typical of spherultic textures, such as those formed by PEO homopolymer.

Table 1. Summary of DSC and SAXS Results on P(EO-*b*-BD) Block Copolymer Samples Crystallized Isothermally at Various Temperatures[a]

T_c (°C)	T_m [a](°C)	T_m [b](°C)	ΔH (J/g)	L_0 (nm)	L_{PEO} (nm)
34	52.1	52.7	165	21.5	10.3
38	52.2	42.8	163	21.6	10.4
40	52.4	52.9	162		
42	52.6	53.1	165	22.4	10.8
44	52.8	53.4	165		
46	53.0	53.6	167	23.2	11.1
48	53.3	53.8	169	23.8	11.4
49	53.5	54.1	167		
50	53.7	54.3	169	24.9	12.0
51	53.9	54.6	167		

[a] T_c = isothermal crystallization temperature; T_m[a] = onset temperature of the primary melting peak; T_m[b] = peak temperature of the primary melting peak; ΔH = heat of fusion, normalized to the weight of PEO in the block copolymer; L_0 = lamellar domain spacing measured by SAXS; L_{PEO} = PEO crystalline chain length calculated based on volume fraction and percentage crystallinity.

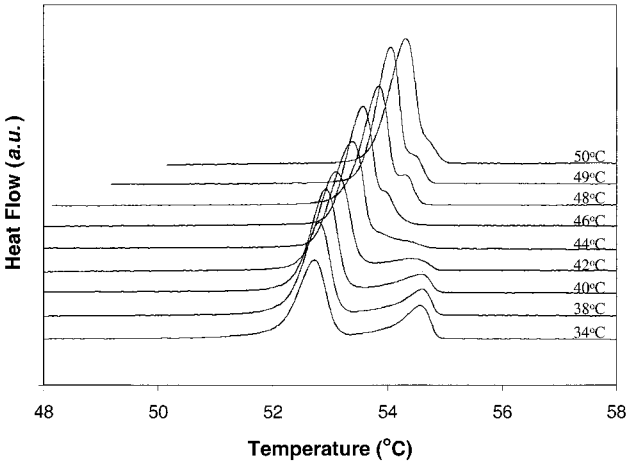

Figure 5. DSC melting endotherms of P(EO-*b*-BD) after isothermal crystallization at the various crystallization temperatures indicated.

Similar lack of the Maltese cross pattern has been previously reported by Wittmann et al. in the study of poly((ethylene oxide)-*b*-styrene) (P(EO-*b*-S)) block copolymers,[35] where it was termed *pseudomorphosis*. Psudomorphosis is a term originally meant to describe crystallization confined within a preexisting liquid crystalline texture.[36] We conducted similar optical microscopy studies on P(EO-*b*-BD) samples crystallized at temperatures ranging from 20 to 50 °C. The effect of crystallization temperature on block copolymer grain structure is beyond the scope of the current paper, but the results observed at all temperatures were qualitatively similar to those reported here.

The crystallization characteristics of PEO in the block copolymer were investigated by DSC and SAXS. Results including T_m, ΔH, and domain spacing l of the samples crystallized at various temperatures (T_c) are summarized in Table 1. Figure 5 shows the DSC heating curves for the P(EO-*b*-BD) block copolymer crystallized isothermally between 30 and 50 °C. The DSC heating rate was 1 °C/min. Crystallization temperatures of 52 °C or higher do not produce observable crystallinity even after an extended period of time and with the use of self-seeding methods. ΔH was found to be essentially independent of T_c. Using the heat of fusion for an infinite, perfect PEO crystal ($\Delta H_f°$) obtained by Buckley and Kovacs[37] via extrapolation of experimental results

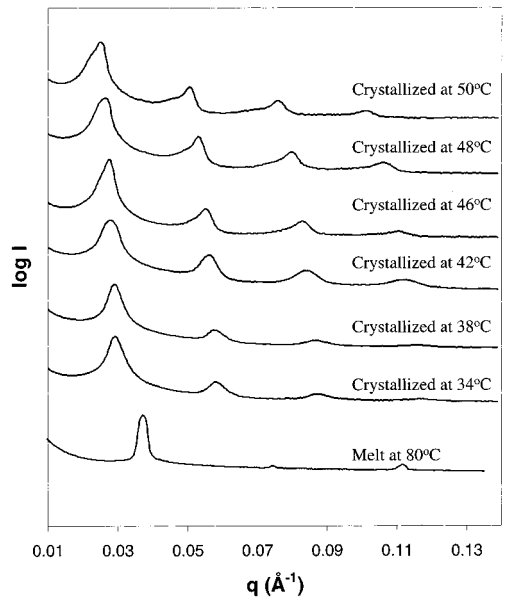

Figure 6. SAXS data for P(EO-*b*-BD) in both the molten and crystalline states. Crystallization conditions as indicated.

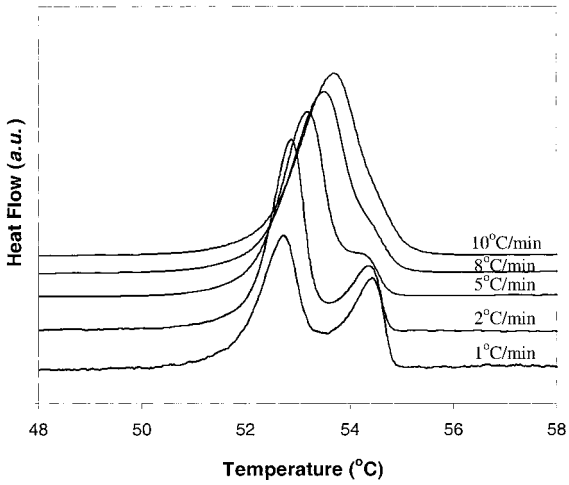

Figure 7. Effect of heating rate on DSC melting endotherms.

on PEO homopolymer (188.9 J/g), the degree of crystallinity of PEO in P(EO-*b*-BD) was about 88%.

For isothermal crystallization below 44 °C, the subsequent heating curves (Figure 5) show two melting endotherms. The first peak has an onset temperature at 52.2 °C while the onset temperature of the second peak is at 54 °C. The position of the second melting endotherm does not change noticeably as the crystallization temperatures varies from 34 to 42 °C. This indicates that this higher temperature endotherm may correspond to a population of integrally folded crystallites. Figure 7 shows a series of heating curves for samples all crystallized at 34 °C but subject to different heating rates in the DSC. As the heating rate increases, the ratio of the first peak to the second peak increases dramatically. Therefore, it can be concluded that these higher melting crystallites were not formed during the initial crystallization process. Instead, they result from thickening of the existing crystallites during heating in the DSC. At higher heating rates, there is less time for crystallite thickening, and the area under the higher melting peak decreases. With decreasing degree of undercooling, as shown in Figure 5, the intensity of the second melting peak decreased, indicating less crystallite thickening.

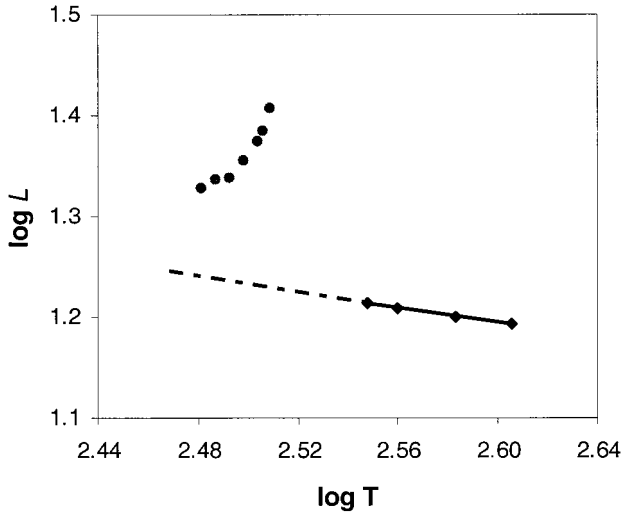

Figure 8. Lamellar long spacing as a function of temperature: (◆) samples in the molten state; (●) samples in the crystalline state.

Figure 6 shows SAXS data for the block copolymer in the molten and crystalline states. The samples were prepared in the DSC instrument at different isothermal crystallization temperatures. The lamellar long period in the melt at 80 °C is 16.4 nm. Figure 8 is a plot of experimentally measured P(EO-*b*-BD) lamellar repeat spacings (l) as a function of temperature (T) in the molten state. From the plot, l was found to scale as $T^{-0.35}$, which agrees closely with the theoretically predicted[38] scaling of $T^{-1/3}$. Taking this temperature effect into consideration, a hypothetical P(EO-*b*-BD) sample in the molten state at 34 °C would have a domain spacing of 17.2 nm. The crystallization of the PEO blocks results in an increase in lamellar long period of about 4 nm over the lamellar spacing of the hypothetical amorphous system at 34 °C. In the lamellar morphology, the thickness of the PEO crystalline lamellae can be calculated by multiplying the long period by the PEO volume fraction. The volume fraction of crystalline PEO in the block copolymer, considering 88 wt % crystallinity, is about 48%. Therefore, the calculated PEO crystalline lamellar fold length, when crystallized at 34 °C, is about 10.5 nm. PEO homopolymer is known to crystallize in a 7_2 helical structure with a chain axis repeat distance of 1.95 nm,[28] corresponding to 0.28 nm per monomer unit. Thus, the fully extended, crystalline chain length of our 5600 g/mol PEO blocks is about 35.6 nm. Consequently, the PEO blocks crystallized at 34 °C are folded to produce at least three chain stems per molecule.

For T_c higher than 46 °C, a small shoulder appeared at higher T_m in the DSC melting curves shown in Figure 5. The SAXS data in Figure 6 show a corresponding lower q shoulder on the Bragg peaks, indicating the presence of a minority population of thicker crystallites in the samples crystallized at 46, 48, and 50 °C. Both the T_m and the size of the crystals corresponding to these small shoulders increased with increasing T_c. This suggests another population of nonintegral folded crystallites but with a slightly larger fold length. This phenomenon has been previously reported by Cheng and co-workers,[39] where it was suggested that it might be

related to fluctuations in the fold length of the initial nuclei.

Discussion

TEM observation of block copolymer grain structure and the absence of spherultic texture in optical micrographs indicate that crystallization occurs within the confinement imposed by the preexisting microphase-separated morphology. Because of the flexibility of the amorphous PBD block in P(EO-*b*-BD), thickening of the PEO domains can occur upon crystallization (Figure 8) without major disruption of the microphase-separated lamellar organization. This behavior is in contrast to that of poly((ethylene oxide)-*b*-styrene)[20,21] or poly-(ethylene-*b*-styrene)[8,40] block copolymers, where the rigid PS domain prohibits any dimensional change of the morphology during crystallization.

TEM and electron diffraction indicate that the model shown in Figure 1 is fairly representative of the P(EO-*b*-BD) structure. The amorphous PBD blocks and crystalline PEO blocks share a common interfacial area per chain. Increasing the thickness of the crystalline lamellae will decrease the area per diblock at the P(EO-*b*-BD) interface and thus will cause stretching of the amorphous PBD chains. The interaction between an enthalpic driving force to minimize the fold surface energy and the entropic term from stretching of the amorphous chains will result in an equilibrium structure which has folded chain crystallites. This clearly differs from the equilibrium structure of homopolymers where the extended chain crystals are the most stable species. However, crystallization is heavily influenced by kinetics, and the equilibrium state often cannot be achieved experimentally. However, analysis of a series of data taken at decreasing undercoolings, of the type presented here, can be used to estimate properties of the equilibrium structure.

The crystallization and melting behavior of PEO homopolymer have been extensively studied.[37,39,41−44] For low molecular weight PEO, crystallites with an integral number of folds are much more stable than nonintegral folded crystallites, and thus nonintegral folded chains will transform to integral folded crystals via isothermal thickening or thinning processes.[24,39] As a result, the DSC heating curves of low molecular weight PEO usually consist of multiple melting endotherms corresponding to different populations of PEO crystallites with different integral fold numbers.[37] Changing the undercooling results in stepwise changes in crystallite thickness from one integrally folded state to another and in several distinctively different melting temperatures (T_m) as a function of different isothermal crystallization temperature (T_c).

In the present study, monotonically increasing melting temperatures with decreasing degrees of undercooling were observed, suggesting that the thickness of the folded chain crystals changed continuously. The DSC results were consistent with the SAXS measurements, where a continuous increase in lamellar spacing with decreasing undercooling was observed. The T_m and long period are plotted vs T_c in Figure 9. The results clearly indicate that for P(EO-*b*-BD) block copolymers that the PEO fold lengths and the corresponding melting temperatures are T_c dependent and that there does not appear to be a special preference for integral folding of PEO crystalline chains.

The equilibrium melting temperature (T_m*) of a polymer can be estimated by the Hoffman−Weeks method.[45] Extrapolating the measured T_m vs T_c curve to $T_m = T_c$, assuming a constant thickening ratio (β) with respect to the initial nuclei, results in $T_m^* \sim 54.8$ °C, which is much lower than the equilibrium melting temperature (64 °C) of 6000 g/mol PEO homopolymer.[37] This method allows for some estimation of T_m*. However, strictly speaking, the Hoffman−Weeks extrapolation is only suitable for homopolymers because it does not consider the entropic contribution of the amorphous block. In addition, using the Hoffman−Weeks extrapolation, we cannot obtain the equilibrium lamellar spacing.

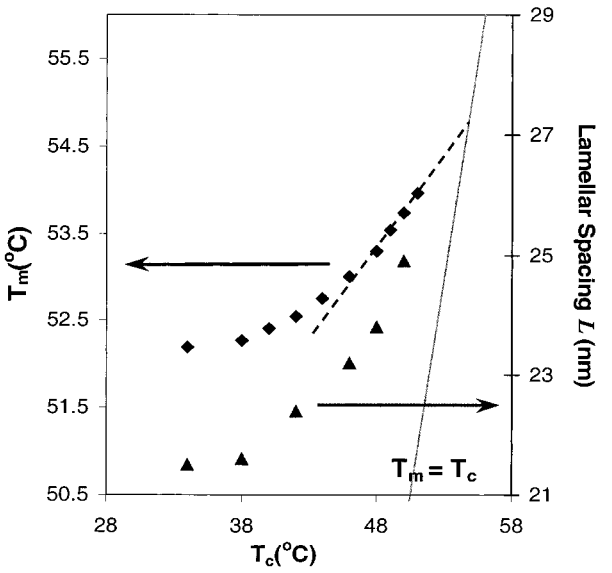

Figure 9. Melting temperature (T_m) and lamellar long period dependence on the crystallization temperature (T_c). The $T_m = T_c$ line is also shown in the plot. The dash line is the extrapolation of the experimental T_m data to $T_m = T_c$ based on the Hoffman−Weeks method.

A thermodynamic analysis of the melting process of the P(EO-*b*-BD) block copolymers is carried out, which assumes equilibrium and thus equates the chemical potentials of the system in the molten and crystalline states at T_m. The Gibbs free energy in the crystalline state is the sum of the contributions from the interfacial energy between PEO and PBD, the conformational energy of the amorphous PBD chains, and the enthalpy and entropy changes on the formation of crystalline PEO. The Gibbs free energy in the melt is the sum of the contributions from the interfacial energy between PEO and PBD in the molten state and the conformational energies of amorphous PEO and PBD chains. Equating chemical potentials and simplifying, the following relationship between melting temperature (T_m) and morphological structure is obtained:

$$T_m = \frac{N_{PEO}\Delta H_f^o - \left(\frac{\tilde{v}_{PBD}}{L_{PBD}}\gamma_c - \frac{\tilde{v}_{PBD}}{l_{PBD}}\gamma_a\right)}{N_{PEO}\frac{\Delta H_f^o}{T_m^o(\infty)} + \left(\frac{\pi^2}{16}\left(\frac{L_{PBD}^2}{R_{PBD}^2} - \frac{l_{PBD}^2}{R_{PBD}^2}\right) - \frac{\pi^2}{16}\frac{l_{PEO}^2}{R_{PEO}^2}\right)R^*} \quad (1)$$

In this equation, for component i, N_i is the degree of polymerization, $\tilde{v}_i$ is the molar volume of segments, and R_i is the unperturbed chain dimension. The brush

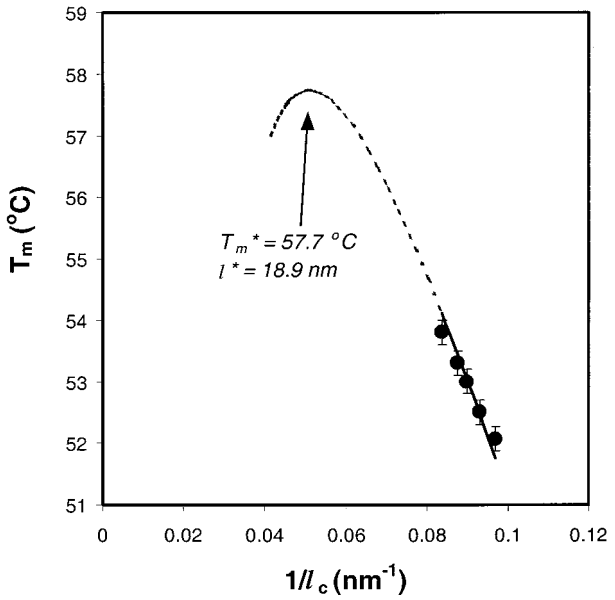

Figure 10. T_m dependence on the reciprocal of crystalline lamellar thickness ($1/L_{PEO}$) of the PEO blocks in P(EO-*b*-BD) block copolymers. The solid line is a fit of eq 1 to the experimental data (●), and the dash line represents the theoretical model embodied in eq 1 with the interfacial energy parameter obtained by fitting the experimental data.

heights for component i in the crystalline and melt states are L_i and l_i, respectively. The interfacial energies between the PEO and PBD in the crystalline and amorphous states are γ_c and γ_a, respectively. The heat of fusion of a perfect, infinitely thick PEO homopolymer crystal is $\Delta H_f°$, and its melting temperature is $T_m°(\infty)$. The universal gas constant is R^*. The difference between eq 1 and the derivation of Ashman and Booth[46] is that eq 1 applies to melting from a semicrystalline structure into a microphase-separated state while the Ashman and Booth model melts into a homogeneous, non-microphase-separated state.

L_{PBD}, l_{PBD}, and l_{PEO} were obtained from SAXS measurements of the lamellar long period and a knowledge of component volume fractions. The interfacial free energy in the melt state γ_a is estimated[47] to be about 1.7 kT/nm^2. The typical interfacial energy for fully amorphous, microphase-separated block copolymers[34] such as poly(styrene-*b*-butadiene) is on the order of 1 kT/nm^2. The interfacial free energies in the crystalline state, γ_c, are difficult to measure. However, eq 1 can be fitted to an experimentally determined plot of T_m vs L_{PEO} using γ_c as an adjustable parameter. The plot is shown in Figure 10. The solid line gives the fitted curve in the region were experimental data are available; this fitting provides an estimate of the interfacial energy in the crystalline state: $\gamma_c \approx 16\ kT$/nm^2. For comparison, the surface energy of homopolymer PEO crystallites in a PEO melt was reported to be 7.5 kT/nm^2 by Buckley and Kovacs.[37] The crystal/amorphous interfacial energy as obtained by Ashman and Booth[46] for a miscible PEO/PPO block copolymer system is about 4.4 kT/nm^2. Presumably, our value of γ_c is higher because it results from both the difference between crystalline and amorphous material and a difference in chemistry between PEO and PBD. Our results, considering the simplicity of the treatment, are in good agreement with previously reported data.

The dashed part of the curve in Figure 10 represents the theoretical model embodied in eq 1 with the interfacial energy parameters obtained by fitting the experimental data. This curve shows a maximum at $T_m = 57.7$ °C. This indicates that in a crystalline/amorphous block copolymer, if the crystalline lamellar thickness becomes longer than a limiting value (18.9 nm), the melting temperature of the structure is reduced as unfavorable stretching of the amorphous chains begins to dominate. Consequently, the maximum in T_m corresponds to the melting temperature of crystalline/amorphous block copolymers in their most stable state. Thus, the equilibrium thickness for the crystalline PEO block is about 18.9 nm. In addition, the equilibrium melting temperature of the P(EO-*b*-BD) studied in this report is estimated to be 57.7 °C, which is a considerable depression relative to that of PEO homopolymer of the same molecular weight. SAXS results in Figure 8 indicate that the amorphous PBD chains are considerably more stretched when the PEO block is crystallized than when the PEO block is in the melt state. Thus, melting of PEO block of the copolymer will release entropic energy stored in the amorphous chain, further depressing the observed melting point. Consequently, the observed decrease of the P(EO-*b*-BD) melting point relative to PEO homopolymer results from a reduction of both the crystalline thickness and the entropy of stretched amorphous chains.

Conclusions

The morphology of a symmetric block copolymer P(EO-*b*-BD) was found via TEM and electron diffraction to consist of strictly alternating PEO and PBD layers with PEO crystalline chain oriented normal to the microphase-separated domain interface. Optical microscopy indicated that the confinement of PEO by the microphase-separated structure suppressed the formation of spherulitic texture during crystallization. The PEO block was found to have a high crystallinity, about 88%. Thus, the structure of this block copolymer in the solid state can be best described by the theoretical model proposed previously.[2,5] The crystallization of PEO in the diblocks results in nonintegral folded crystallites, and chain stretching energy in the amorphous blocks prevents the formation of extended chain PEO crystallites.

By using the methods discussed in this paper, melting temperature and structural information on the equilibrium state of P(EO-*b*-BD) can be obtained. This study only utilized a single block copolymer of given molecular weight. To study the scaling behavior of the equilibrium state for these systems, for comparison to theory, this work would need to be extended to encompass a series of samples of varying molecular weights. The present work indicates that the P(EO-*b*-BD) system is a good model system in achieving such a task.

Acknowledgment. Work at the University of Massachusetts Amherst was supported by the Materials Research Science and Engineering Center (MRSEC) under NSF Grant DMR9809365. Helpful discussions with T. P. Russell are also acknowledged.

References and Notes

(1) DiMarzio, E. A.; Guttman, C. M.; Hoffman, J. D. *Macromolecules* **1980**, *13*, 1194.
(2) Whitmore, M. D.; Noolandi, J. *Macromolecules* **1988**, *21*, 1482.
(3) Vilgis, T.; Halperin, A. *Macromolecules* **1991**, *24*, 2090.
(4) Noshay, A.; McGrath, J. E. *Block Copolymer, Overview and Critical Survey;* Academic Press: New York, 1977.

(5) Douzinas, K. C.; Cohen, R. E.; Halasa, A. F. *Macromolecules* **1991**, *24*, 4457.
(6) Hamley, I. W.; Fairclough, J. P. A.; Bates, F. S.; Ryan, A. J. *Polymer* **1998**, *39*, 1429.
(7) Kofinas, P.; Cohen, R. E. *Macromolecules* **1994**, *27*, 3002.
(8) Cohen, R. E.; Cheng, P. L.; Douzinas, K.; Kofinas, P.; Berney, C. V. *Macromolecules* **1990**, *23*, 324.
(9) Sakurai, K.; MacKnight, W. J.; Lohse, D. J.; Schulz, D. N.; Sissano, J. A.; Lin, J. S.; Agamalyan, M. *Polymer* **1996**, *37*, 4443.
(10) Hamley, L. W.; Fairclough, J. P. A.; Terrill, N. J.; Ryan, A. J.; Lipic, P. M.; Bates, F. S.; Towns-Andrews, E. *Macromolecules* **1996**, *29*, 8835.
(11) Quiram, D. J.; Register, R. A.; Marchand, G. R.; Adamson, D. H. *Macromolecules* **1998**, *31*, 4891.
(12) Hong, S.; Bushelman, A. A.; MacKnight, W. J.; Gido, S. P.; Lohse, D. J.; Fetter, L. J. *Polymer* **2001**, *42*, 5909.
(13) Rangarajan, P.; Register, R. A.; Fetters, L. J. *Macromolecules* **1993**, *26*, 4640.
(14) Loo, Y. L.; Register, R. A.; Ryan, A. J. *Phys. Rev. Lett.* **2000**, *84*, 4120.
(15) Gervais, M.; Gallot, B. *Makromol. Chem.* **1973**, *174*, 193.
(16) Mai, S.; Fairclough, J. P. A.; Hamley, I. W.; Matsen, M. W.; Denny, R. C.; Liao, B.; Booth, C.; Ryan, A. J. *Macromolecules* **1997**, *30*, 8392.
(17) Ryan, A. J.; Hamley, I. W.; Bras, W.; Bates, F. S. *Macromolecules* **1995**, *28*, 3860.
(18) Ryan, A. J.; Fairclough, J. P. A.; Hamley, I. W.; Mai, S.; Booth, C. *Macromolecules* **1997**, *30*, 1723.
(19) Nojima, S.; Kato, K.; Yamamoto, S.; Ashida, T. *Macromolecules* **1992**, *25*, 2237.
(20) Zhu, L.; Chen, Y.; Zhang, A.; Calhoun, B. H.; Chun, M.; Quirk, R. P.; Cheng, S. Z. D.; Hsiao, B. S.; Yeh, F.; Hashimoto, T. *Phys. Rev. B* **1999**, *60*, 10022.
(21) Zhu, L.; Cheng, S. Z. D.; Calhoun, B. H.; Ge, Q.; Quirk, R. P.; Thomas, E. L.; Hsiao, B. S.; Yeh, F. J.; Lotz, B. *J. Am. Chem. Soc.* **2000**, *122*, 5957.
(22) Kovacs, A. J.; Gonthier, A. *Kolloid Z. Z. Polym.* **1972**, *250*, 530.
(23) Buckley, C. P.; Kovacs, A. J. *Prog. Colloid Polym. Sci.* **1975**, *58*, 44.
(24) Cheng, S. Z. D.; Zhang, A.; Chen, J.; Heberer, D. P. *J. Polym. Sci., Polym. Phys. Ed.* **1991**, *29*, 287.
(25) Hong, S.; MacKnight, W. J.; Russell, T. P.; Gido, S. P. *Macromolecules* **2001**, *34*, 2398.
(26) Hong, S.; MacKnight, W. J.; Russell, T. P.; Gido, S. P. *Macromolecules*, in press.
(27) Reiter, G.; Castelein, G.; Hoerner, P.; Riess, G.; Sommer, J. U.; Floudas, G. *Euro. Phys. J. E* **2000**, *2*, 319.
(28) Brandrup, J.; Immergut, E. H. *Polymer Handbook;* Interscience: New York.
(29) Gido, S. P.; Thomas, E. L. *Macromolecules* **1994**, *27*, 6137.
(30) Gido, S. P.; Gunther, J.; Thomas, E. L.; Hoffman, D. *Macromolecules* **1993**, *26*, 4506.
(31) Newstein, M. C.; Garetz, B. A.; Dai, H. J.; Balsara, N. P. *Macromolecules* **1995**, *28*, 4587.
(32) Gido, S. P.; Schwark, D. W.; Thomas, E. L.; Goncalves, M. *Macromolecules* **1993**, *26*, 2636.
(33) Gido, S. P.; Thomas, E. L. *Macromolecules* **1994**, *27*, 849.
(34) Burgaz, E.; Gido, S. P. *Macromolecules* **2000**, *33*, 8739.
(35) Wittmann, J. C.; Lotz, B.; Candau, F.; Kovacs, A. J. *J. Polym. Sci., Polym. Phys. Ed.* **1982**, *20*, 1341.
(36) Friedel, G. *Ann. Phys. (Paris)* **1922**, *18*, 273.
(37) Buckley, C. P.; Kovacs, A. J. *Kolloid Z. Z. Polym.* **1976**, *254*, 695.
(38) Hamley, I. W. *The Physics of Block Copolymers;* Oxford University Press: Oxford, 1998.
(39) Cheng, S. Z. D.; Zhang, A.; Barley, J. S.; Chen, J.; Habenschuss, A.; Zschack, P. R. *Macromolecules* **1991**, *24*, 3937.
(40) Douzinas, K. C.; Cohen, R. E. *Macromolecules* **1992**, *25*, 5030.
(41) Kovacs, A. J.; Straupe, C.; Gonthier, A. *J. Polym. Sci., Polym. Symp.* **1977**, *59*, 31.
(42) Alfonso, J. C.; Russell, T. P. *Macromolecules* **1986**, *19*, 1143.
(43) Cheng, S. Z. D.; Bu, H. S.; Wunderlich, B. *J. Polym. Sci., Polym. Phys. Ed.* **1988**, *26*, 1947.
(44) Cheng, S. Z. D.; Wu, S. S.; Chen, J.; Zhuo, Q.; Quirk, R. P.; Meerwall, E. D. V.; Hsiao, B. S.; Habenschuss, A.; Zschack, P. R. *Macromolecules* **1993**, *26*, 5105.
(45) Gedde, U. W. *Polymer Physics;* Chapman & Hall: New York, 1995.
(46) Ashman, P. C.; Booth, C. *Polymer* **1975**, *16*, 889.
(47) Floudas, G.; Ulrich, R.; Wiesner, R. *J. Chem. Phys.* **1999**, *110*, 652.

MA0100596